DOI: 10.15669/pnst.8.171

Progress in Nuclear Science and Technology
Volume 8 (2025) pp. 171-175

ARTICLE

Study of Heat Transfer Performance for Sodium-Molten Salt Heat Exchanger in Sodium-Cooled Fast Reactor Coupled to Thermal Energy Storage System

Masaaki HAYASHI [1*], Shota SHIRAKURA [1] and Hidemasa YAMANO [2]

[1] *Hitachi-GE Nuclear Energy, Ltd., 1-1, Saiwai-cho 3-chome, Hitachi-shi, Ibaraki 317-0073, Japan*
[2] *Japan Atomic Energy Agency, 4002 Narita-cho, Oarai-machi, Higashiibaraki-gun, Ibaraki-ken, 311-1393, Japan*

For sodium-cooled fast reactor coupled to thermal energy storage (TES) system with sodium–molten salt heat exchanger (HX), Computational Fluid Dynamics (CFD) thermal analyses by STAR-CCM+ with partial HX model are performed as well as simple evaluation of heat transfer performance using heat transfer coefficient formula in this paper. The performance evaluation for a HX with sodium and molten salt confirmed heat transfer improvement measures effects.

KEYWORDS: sodium-cooled fast reactor, thermal energy storage, sodium, molten salt, heat exchanger, STAR-CCM+, CFD thermal analysis

I. Introduction

Next-generation innovative reactors have a new value of their flexibility with variable renewable energy, in addition to safety and economic competitiveness.[1)] A sodium-cooled fast reactor (SFR) can make flexibility by coupling a thermal energy storage (TES) system with molten salt. The TES technology is advantageous to achieve a large-capacity energy storage, in terms of flexibility and cost.[2)] A development element unique to the SFR with TES is a heat exchanger (HX) between sodium and molten salt. There is no information regarding its HX.

In the United States, TerraPower is building Natrium plant near the site of a retiring coal facility in Kemmerer, Wyoming, which combines SFR with TES. Natrium's rated output is 345 MWe and TES can boost the system's output to 500 MWe for more than five and a half hours when needed, giving it the flexibility to coexist with renewable energy sources that have large output fluctuations. There are extensive experiences of Sodium/Sodium HX in SFRs and molten salt HXs in solar thermal power generation, but no experience with Sodium/Molten Salt HXs. The purposes of this study are to improve the accuracy of heat transfer performance evaluation technology and to confirm the effects of heat transfer improvement measures based on STAR-CCM+ CFD thermal analyses results for Sodium/Molten Salt HXs.

II. Heat Transfer Performance Evaluation of HX

Joyo MK-III Intermediate Heat Exchanger (IHX) shown in **Fig. 1** is selected as a reference sodium/sodium HX in this study because the heat transfer performance evaluation results are described in the performance test report.[3)] **Table 1** shows the results of heat transfer performance evaluation using a simple formula. Reference Case is Joyo IHX. In Case 1, the sodium in the tube side is replaced with Solar Salt ($NaNO_3$-KNO_3: 60-40wt.%). In Case 2, the fluid in the shell side and tube side are exchanged and Solar Salt in the shell side is allowed to crossflow around the tubes. The physical properties of Solar Salt are taken from ASME TES-1,[4)] and

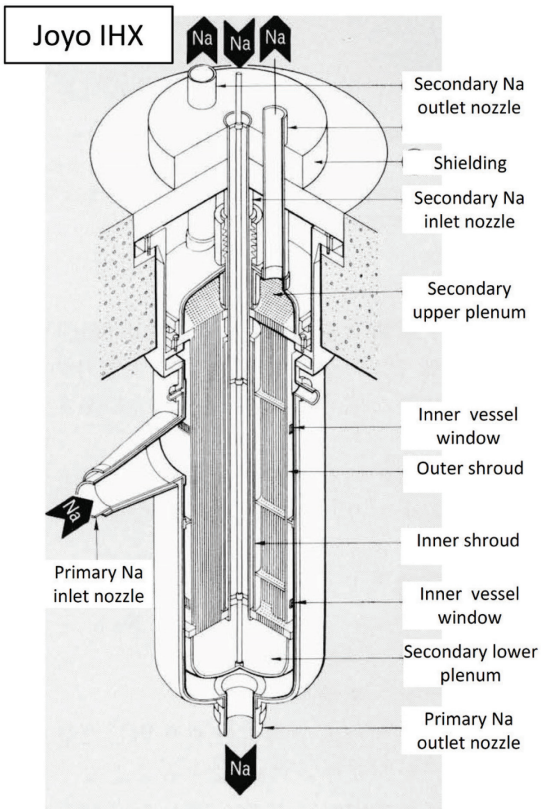

Fig. 1 Joyo IHX Bird-eye View [6)]

*Corresponding author, E-mail: masaaki.hayashi.ak@hitachi.com

the physical properties of sodium are taken from the Sodium Technology Handbook.[5)]

Table 2 shows some physical properties of Solar Salt and sodium at 300°C, 400°C, 500°C. Solar Salt's density is about twice that of sodium and its specific heat is slightly greater than that of sodium. Its melting temperature is approximately 238°C. Solar Salt is used in solar thermal power generation business all over the world because of its good properties in terms of required functions for thermal storage. It is stable heat storage medium in 300-500°C and also good in terms of cost. On the other hand, the thermal conductivity of Solar Salt is less than 1/100 that of sodium. It makes HX sizing design difficult. This increases the required heat transfer area of Case 1 approximately 5.5 times compared with the Reference Case and the HX becomes large.[6)] Various measures to reduce the required heat transfer area are evaluated and it is found that the most effective case is Case 2 which is a shell-and-tube HX with sodium inside tubes and Solar Salt crossflow outside tubes. The required heat transfer area is reduced to 1.7 times that of the Reference Case.[6)]

Table 1 Results of heat transfer performance of HX[6)]

Case	Heat transfer area	Ratio
Reference Case	329 m^2	1.0
Case 1	1801 m^2	5.5
Case 2	563 m^2	1.7

Table 2 Physical properties of Solar Salt and sodium[6)]

Temp. °C	Fluid	Density kg/m^3	Specific Heat J/kgK	Thermal Conductivity W/m^2K
300	Solar Salt	1898	1499	0.500
	Sodium	880	1305	77.1
400	Solar Salt	1834	1516	0.520
	Sodium	856	1279	72.2
500	Solar Salt	1770	1534	0.539
	Sodium	832	1262	67.3

III. HX CFD Thermal Analysis Result

The HX CFD thermal analyses are performed to improve the accuracy of heat transfer performance evaluation technology. **Figure 2** shows the CFD thermal analysis model of Case 3 and Case 4. It is a partial model with 10 layers tubes and four-stage crossflow paths to check the flow pattern and heat transfer performance. This analysis model partially modeled the Case 2 HX tube bundle, which has 18 layers tubes and seventeen-stage crossflow paths. Inlet flow velocities of sodium and Solar Salt in Case 3 are the same as Case 2 in Table 1. The flow velocities of sodium and Solar Salt in Case 4 are 2 times that of Case 3 to check flow velocity effect. The CFD thermal analyses code is STAR-CCM+. The turbulence model is Realizable k-ε and wall treatment is Two-Layer All y+. The thickness of the elements near the surface of the heat transfer tube used in the analysis is appropriately set taking into account the wall function (y+<30). The mesh diagram of analysis model is shown in the bottom of Fig. 2. For example, the analysis model of Case 3 has approximately 2.5 million meshes. HX tube outer diameter is 19 mm and thickness is 1 mm. The tube pitch ratio is 1.25 (Triangular Array). The HX tube material is type 316 stainless steel and the baffle plate distance is 300 mm.

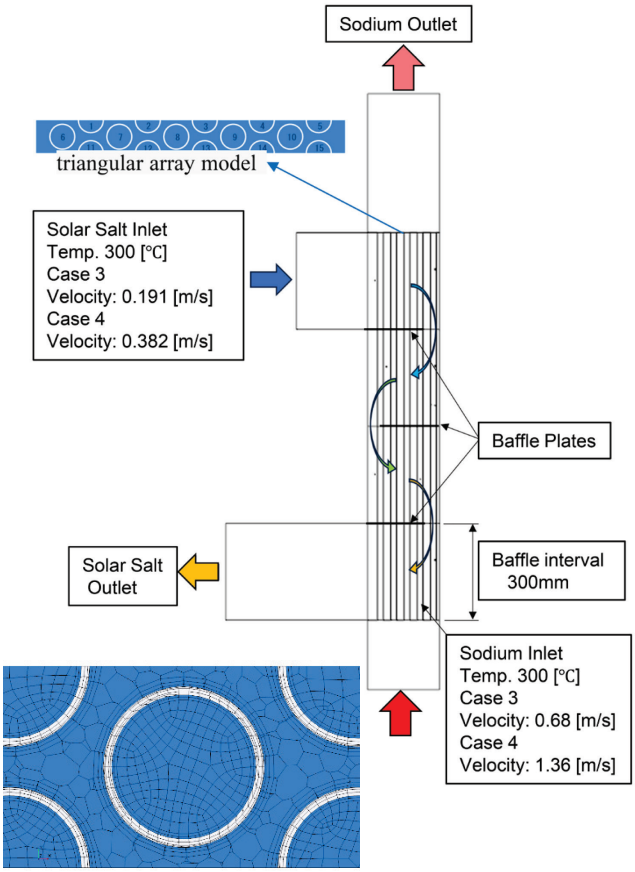

Fig. 2 CFD thermal analysis model

Figure 3 shows Velocity Distribution of Case 3 and Case 4. Sodium flows into the HX tubes from the bottom of the model at 500°C, and its temperature gradually decreases before flowing out from the top. The Solar Salt that entered the outside of the tube bundle from the upper side of the model at 300°C rises in temperature each time it passes through crossflow, and flows out from the lower side of the model. Velocity Distribution at the cross section AA is shown. Vortices are generated in the wake of the baffle plate at the turning point of the cross flow on the Solar Salt side. Locations of vortices are marked by red rectangular in Fig. 3.

Figure 4 shows Temperature Distribution of Case 3 and Case 4. Temperature Distribution at the cross section AA is shown. In the vortex area, the flow rate of Solar Salt becomes slower, and the temperature rises more than in other areas.

Figure 5 shows Velocity Vector of Case 3 analysis results in the second crossflow. **Figure 6** shows Velocity Vector of

Case 4 analysis results in the second crossflow. In the Solar Salt side, flow vortices enclosed in red squares are observed. The strong downward flow from the window of the baffle plate causes a backflow vortex behind the baffle plate. As indicated by the color of the arrow, their velocity is very small, and they adversely affect heat transfer performance. These flow vortices are also observed in the third and the fourth crossflows of Case 3 and Case 4.

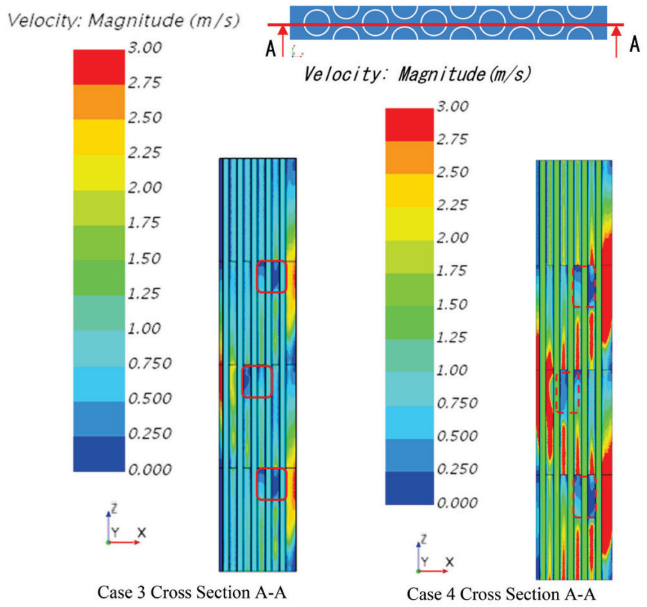

Fig. 3 Velocity distribution of Case3 and Case 4

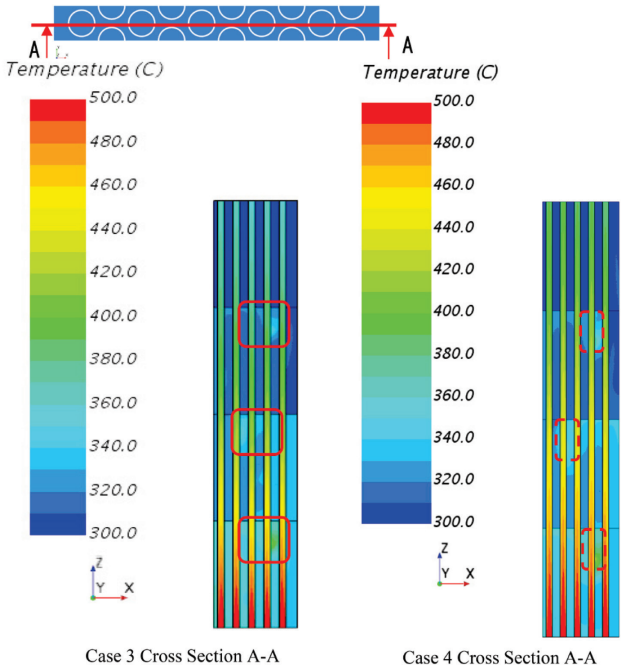

Fig. 4 Temperature distribution of Case3 and Case 4

IV. Heat Transfer Evaluation

Table 3 shows Comparison of heat transfer coefficient in sodium side. Temperature and velocity used in the evaluation

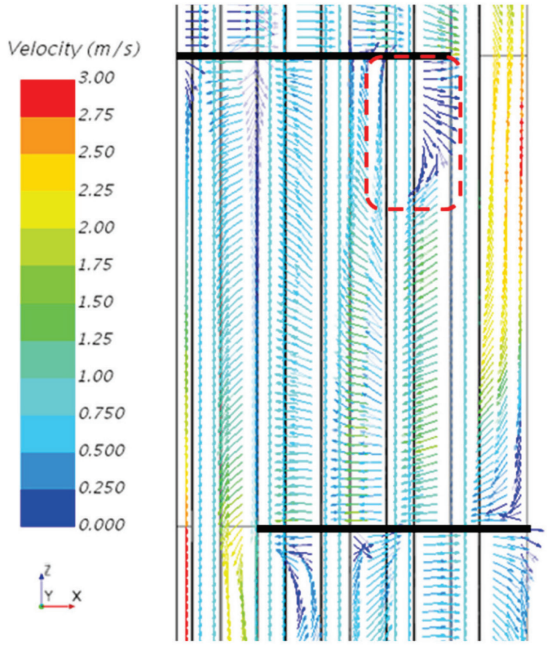

Fig. 5 Velocity Vector of Case3

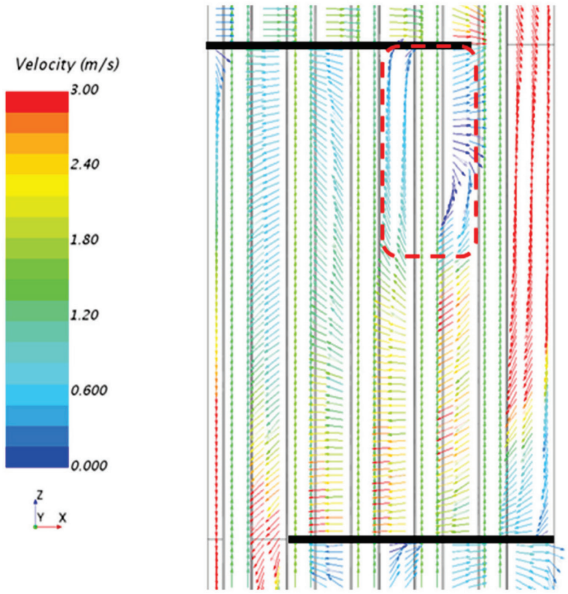

Fig. 6 Velocity Vector of Case 4

are the same as those shown in Fig. 2. The heat transfer coefficient can be calculated by multiplying Nu by the thermal conductivity and dividing it by the outer diameter of the tube. Heat transfer equations of Lubarsky-Kaufman, Subbotin and Martinelli Lyon and analysis results are compared. The values increase in the order of Lubarsky-Kaufman,[7] Subbotin.[7,8] and Martinelli Lyon[7] and Martinelli Lyon and the analysis results match well. The Lubarsky-Kaufman equation is applied to the sizing of heat exchangers as a conservative evaluation because the heat transfer coefficient becomes smaller when the Lubarsky-Kaufman equation is used. The Lubarsky-Kaufman equation is also used for the heat exchanger in the Reference Case. Designing using the Lubarsky-Kaufman equation might be overly conservative, so it is advisable to

review the heat transfer coefficient equation based on the Joyo MK-III IHX performance test report,[3] etc.

Case 4 doubled the flow rate compared to Case 3, but the heat transfer coefficient only increased by about 16%. On the other hand, pressure loss has increased significantly.

From the STAR CCM+ CFD thermal analysis results in a steady state, the volumetric average temperature of the fluid per heat transfer tube, the average temperature on the heat transfer tube surface, and the heat flux are provided. The heat transfer coefficient is calculated by dividing the heat flux by the surface area of the heat transfer tube and by the temperature difference between the volumetric average temperature of the fluid and the average temperature on the heat transfer tube surface. The heat transfer coefficients of the analysis results shown in Tables 3 indicate the average value of the heat transfer coefficients calculated for all heat transfer tubes.

Table 3 Comparison of heat transfer coefficient in sodium side [6]

Case	Equations	Nu	Heat transfer coefficient W/m^{2}K	Ratio
Case3	A	4.93	20,300	0.58
	B	6.55	27,000	0.77
	C	8.55	35,300	1.00
	Analysis result	-	36,700	1.04
Case4	A	6.50	26,800	0.67
	B	7.70	31,800	0.80
	C	9.70	40,000	1.00
	Analysis result	-	42,700	1.07

Note: Equations A, B and C are shown in equations (1), (2) and (3).
Ratio: Ratio when heat transfer coefficient compared with Martinelli Lyon equation's

A: Lubarsky-Kaufman equation[7]

$$Nu = 0.625Pe^{0.4} \quad (1)$$

Nu: Nusselt number
Pe: Peclet number

B: Subbotin equation[7, 8]

$$Nu = 5 + 0.025Pe^{0.8} \quad (2)$$

C: Martinelli Lyon equation[7]

$$Nu = 7 + 0.025Pe^{0.8} \quad (3)$$

$$\alpha = Nu \times \frac{\lambda}{L} \quad (4)$$

α: heat transfer coefficient (W/m^{2}K)
λ: thermal conductivity (W/mK)
L: length (inside the tube, the inner diameter of the heat transfer tube; outside the tube, the molten salt side, the outer diameter of the heat transfer tube) (m)

Table 4 shows Comparison of heat transfer coefficient in Solar Salt side. The analysis results are about 20% smaller than the equation of Zukauskas.[7,9] While the equation for Zukauskas is an ideal crossflow equation, the analysis results show uneven flow and vortices, reducing heat transfer. The heat transfer coefficients of analysis results are calculated in the same way as the sodium side.

Counter measures to improve heat transfer are needed.

The heat transfer performance improvement by shell side Solar Salt cross flow was confirmed by CFD thermal analyses.

As shown in Fig. 2, the partial analysis model with 10 layers tubes in radial direction was applied. For real Reference Case tube bundle area, it is possible to layout 18 layers tubes in radial direction. The CFD model with 18 layers tubes model will be applied for the next step. Usually, windows of baffle plates are provided covering 20% of the area. As shown in Fig. 3, the velocity at baffle plate windows is very high. When 18 layers tubes model is applied, the baffle plate windows area is widened based on generally applicable 20% rule, and it is expected to slow down flow velocity at windows of baffle plates and to reduce vortices after baffle plates. And a reduction in pressure loss on the shell side is also expected due to the effect of slowing down the flow through the windows of the baffle plate. Gaps between tubes and baffle plates are not considered in the analysis model shown in Fig. 2. If a gap is taken into consideration, leakage flow occurs, which usually deteriorates heat exchange performance. On the other hand, the flow from the gap is expected to have the effect of suppressing the generation of vortices. These counter measures to reduce vortices after baffle plates will be confirmed by CFD thermal analysis in the next step.

Table 4 Comparison of heat transfer coefficient in Solar Salt side [6]

Case	Equation	Nu	Heat transfer coefficient W/m^{2}K	Ratio
Case 3	Zukauskas	262	7,100	1.00
	Analysis Result	-	5,600	0.79
Case 4	Zukauskas	398	10,800	1.00
	Analysis Result	-	8.700	0.81

Note Ratio: Ratio when heat transfer coefficient compared with Zukauskas equation's. [7, 9]

Zukauskas equation

$$Nu = 0.35(Y/X)^{0.2} Re^{0.6} Pr^{0.36} \quad (5)$$

X: Tube distance in flow direction (m)
Y: Tube distance perpendicular to flow (m)
Re: Reynolds number
Pr: Prandtl number

Table 5 shows Comparison of pressure loss of Solar Salt side.

Case 3 was considered as a structure in which the flow velocity is increased as much as possible in order to increase the heat transfer coefficient on the Solar Salt side, where the

thermal conductivity is very small. Crossflow outside of tubes with 300 mm baffle plates distance were applied for Case 3. Generally, increasing the flow velocity increases the pressure loss. Pressure loss of Analysis result is Case 3 model shown in Fig. 2. This model is a partial model with 10 tubes layers with four-stage crossflow paths. When the required heat transfer area is considered, 18 tubes layers with seventeen-stage crossflow paths are necessary for the full size HX. The analysis results extrapolated the pressure loss from the partial model to the full size. The pressure loss of 'Calculation by Formula' is compared with the analysis results. It is noticed that pressure loss values of 'Calculation by Formula' under full-size conditions are conservative. The design of the HX must balance the improvement of heat transfer rate with the availability of molten salt pumps. Pressure loss of 'Analysis result Extrapolation'

Table 5 Comparison of pressure loss of Solar Salt side [7)]

Case	Analysis result Partial Model	Analysis result Extrapolation	Calculation by Formula
Case 3	49 kPa	376 kPa	899 kPa
Case 4	229 kPa	1,753 kPa	3,129 kPa

Pressure loss of 'Calculation by Formula' is calculated using the following equations. [7)]

$$\Delta P_B = 18.8Re^{-0.2}\frac{1}{2\rho}\times\left(\frac{m0}{AM}\right)^2\frac{NCSLsin\beta}{de0}\left(\frac{SL}{ST}\right)^{0.6}\left(\frac{de0}{ST}\right)^{0.4} \quad (6)$$

$$de0 = \frac{4(STSLsin\beta-\frac{\pi do^2}{4})}{\pi d0} \quad (7)$$

$$Re = \frac{m0de0}{AM\rho v} \quad (8)$$

ΔP_B: Pressure loss (Pa)
Re: Reynolds number shown in equation (8)
ρ: Density (kg/m^3)
m0: mass flow rate (kg/s)
A_M: Minimum crossflow area in the center of HX (m^2)
N_C: Number of tube layers
S_L: Pitch (Triangular array) (m)
S_T: Pitch (Triangular array) (m)
do: Outer diameter of a tube (m)
β: π/3 (Triangular array)
ν: Dynamic Viscosity (m^2/s)

As explained so far, it was found that an external cross flow structure is the most suitable for improving the heat transfer performance of a HX like Case 3. The heat transfer coefficients inside and outside the tubes calculated using the formula were confirmed by CFD thermal analysis as shown in Table 3 and Table 4. The analysis showed that vortices occur in the wake of the baffle plate in the Solar Salt external crossflow, reducing heat transfer performance, so the next step needs to consider countermeasures to reduce vortices and confirm their effectiveness with CFD thermal analysis.

As for validation of CFD analysis, with each new version of STAR-CCM+, a verification suite with simple heat transfer model is released. Though it would be desirable to consider verification work for a complex flow system with a multi-tube bundle in the future.

V. Conclusion

It is confirmed that a shell-and-tube HX with sodium inside tubes and Solar Salt crossflow outside tubes is very effective as heat transfer improvement measure based on STAR-CCM+ CFD thermal analyses results and a heat transfer performance evaluation using heat transfer coefficient formula.

The analysis showed that vortices occur in the wake of the baffle plate in the Solar Salt external crossflow, reducing heat transfer performance, so the next step needs to consider countermeasures to reduce vortices.

The accuracy of heat transfer performance evaluation technology for Sodium/Molten salt HX is improved.

Acknowledgment

This work was supported by MEXT Innovative Nuclear Research and Development Program Grant Number JPMXD0222682675.

References

1) METI, Agency for natural resources and energy, Ongoing nuclear innovation. https://www.enecho.meti.go.jp/about/special/johoteikyo/smr_01.html
2) C. Forsberg, P. Sabharwall, H. D. Gougar, "Heat Storage Coupled to Generation IV Reactors for Variable Electricity from Base- load Reactors: Workshop Proceedings: Changing Markets," Technology, Nuclear- Renewables Integration and Synergisms with Solar Thermal Power Systems, INL/EXT-19-54909 Revision 0 (2019).
3) JAEA, "Joyo MK-III Performance Test Report," JNC TN9410 2005-005 (2005), [in Japanese].
4) ASME, TES-1 Safety Standard for Thermal Energy Storage System: Molten Salt, ASME TES-1 (2020).
5) JAEA, *Sodium Technology Handbook*, JNC TN9410 2005-011 (2005), [in Japanese].
6) H. Yamano, et al., "Development of safety design technologies for sodium-cooled fast reactor coupled to thermal energy storage system with sodium-molten salt heat exchanger," *Proceedings of the 8th International Conference on New Energy and Future Energy Systems (NEFES2023)*, Matsue, Japan (Nov. 21-24, 2023), FES-2986. New Energy and Future Energy Systems, Advances in *Transdisciplinary Engineering*, **45**, 27-34, DOI:10.3233/ATDE231072.
7) JSME, *JSME Data Book: Heat Transfer 5th Edition*, (2009), [in Japanese].
8) V. I.Subbotin, et al., *Atomn. Energ*., **380**,13-10 (1962).
9) A. Zukauskas, Advances in *Heat Transfer*, **8**, 93 (1972).